AIAA 80-0976R

Trailing-Edge Airframe Noise Source Studies on Aircraft Wings

Werner M. Dobrzynski*
Abteilung Technische Akustik, DFVLR, Braunschweig, Federal Republic of Germany

Interaction between unsteady surface flow and wing trailing edges is considered one of the dominant source mechanisms of airframe noise. For the prediction of trailing-edge noise radiation, detailed information on the unsteady-flow behavior close to and at the edge is essential. Therefore, surface pressure measurements were conducted near the wing/flap trailing edge of a business jet aircraft (HFB-320) and a large commercial aircraft (DC-10/30) under realistic flight conditions within a wide range of flight speeds and typical flap deflection angles. The spectral distribution of pressure intensities and coherences were determined and compared to corresponding results from model and glider measurements, respectively. On the basis of integral pressure field coherence dimensions (deduced from measured data), the applicability of the hydrodynamic trailing-edge noise model is evaluated.

Nomenclature

a = ambient speed of sound, m/s
C = flow variable
f = frequency, Hz
L_p = pressure level (ref. 20 N/m^2), dB
l = integral correlation length, m
$\overline{p_F^2}$ = mean square sound pressure, Pa^2
$\overline{p_S^2}$ = mean square surface pressure, Pa^2
q_∞ = freestream dynamic pressure, Pa
r = distance between source and receiver, m
Δs = effective sensor separation distance, m
U_∞ = freestream (flight) velocity, m/s
U_Γ = velocity component of side-edge vortex orthogonal to side-edge and parallel to flap surface, m/s
W = total wetted span, m
x, y, z = Cartesian coordinates with x in streamwise direction, m
x', y', z' = Cartesian coordinates with x' orthogonal to the trailing edge, m
γ^2 = coherence function
δ^* = boundary-layer displacement thickness, m
θ = angle-of-sound radiation in the y-z plane, deg
λ_c = convective hydrodynamic wavelength, m
ξ = relative eddy spacing in spanwise direction
$\phi_{1,2}$ = relative phase angle from cross-power spectrum, deg
ψ = angle of sound radiation in the x-z plane, deg

Introduction

AIRFRAME noise prediction is still largely an empirical art due to the complexity of aircraft geometries and the ensuing flow patterns, particularly when landing-approach configurations are considered. Even for a "classical" noise source such as the wing trailing edge, available theories do not yield accurate results, since the unsteady flow behavior in the very vicinity of the edge is not known to the necessary degree of accuracy even if an infinitely extended "two-dimensional" airfoil is considered. Much less information is available on the flow characteristics near the wing trailing edges of realistic aircraft, particularly in view of the unknown effects of Reynolds numbers (which are high for the real aircraft case) and of the possible vibrational effects on the usually nonrigid surface structure.

Therefore, it seemed important to conduct an experimental program to investigate the flow characteristics near the trailing edges of real, i.e., full-scale, aircraft. This paper describes results of such a program in which a business jet and a large commercial aircraft were used as test vehicles.

Problem Definition

Trailing-edge noise theories and physical ad-hoc models to predict farfield radiated noise have been discussed and were recently extended by Howe.[1] He emphasized again that flow turbulence characteristics as well as the unsteady flow conditions at the very edge are the essential parameters governing the noise radiation from the edge. Appropriate model-scale tests were conducted by Brooks and Hodgson.[2] These investigations showed the lower bound of edge noise—if there was one—and what the influencing parameters were. For full-scale aircraft the contribution of trailing-edge noise to the total airframe noise cannot be extracted by experiment. Therefore, surface pressure measurements and analyses with respect to the unsteady flow characteristics near the trailing edges of real aircraft were considered to be useful to complement the detailed model experiments.

Similar measurements were conducted earlier on a glider wing whereby surface pressure spectra and integral pressure field correlation lengths had been determined[3] and farfield radiated edge noise had been calculated on the basis of the hydrodynamic edge-noise model given by Hayden et al.[4]

Experimental Program

Fluctuating surface pressures were measured near the trailing edges of a business jet, a HFB-320, and of a large commercial aircraft, a DC-10/30 (Fig. 1). Miniature piezoelectric pressure sensors of ¼ in. diam were flush mounted in a specially designed panel of 4 mm thickness on the suction side of each aircraft wing/flap, respectively. A total of seven sensors together with an accelerometer were arranged in a T-shaped array parallel and perpendicular to the respective edge (Fig. 2), whereby a minimum edge distance to within 1% of the chord was achieved. For reference purposes, one additional sensor was located at the spanwise location of the sensor array but at the 30% chord position from the leading edge. On the HFB-320 additional measurements were conducted with a sensor array located at the outer side edge of

Presented as Paper 80-0976 at the AIAA 6th Aeroacoustics Conference, Hartford, Conn., June 4-6, 1980; submitted June 19, 1980; revision received Oct. 20, 1980.

*Senior Scientist.

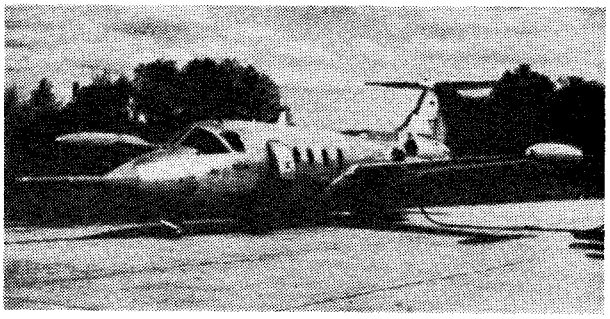

Fig. 1a Business jet aircraft HFB-320.

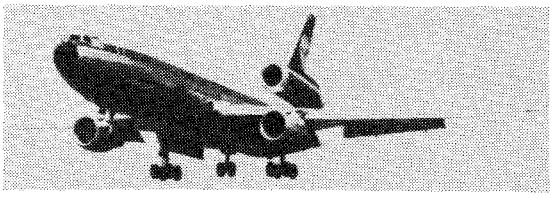

Fig. 1b Commercial aircraft DC-10/30.

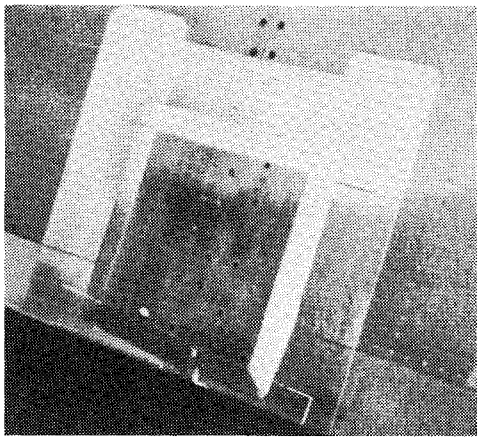

Fig. 2 Sensor array on DC-10/30 flap trailing edge.

the flap since this region is known to be an area of highly disturbed flow when the flap is deployed (Fig. 3).

Data were taken both in the cruise configuration and at different flap deflection angles (typically 20, 35, and 50 deg) and for various flight speeds.

Results

The results pertain to the aircraft at cruise and during landing approach (i.e., with a 50 deg flap deflection angle), representing the two extreme operational conditions. As became evident, small flap deflection angles—as typical for takeoff—do not significantly alter the flow characteristics at the edge compared to those at cruise.

Measured surface pressure data are compared and normalized on the basis of aircraft flight speed and boundary-layer displacement thicknesses calculated for a flat plate at zero pressure gradient. This procedure was applied to both the suction and pressure sides of the airfoil, with the chordwise sensor distance to the airfoil leading edge as the relevant length scale.

Surface Pressure Spectra

Cruise Configuration

In comparing spectra obtained through all 17 measuring locations within 1-5% chord distance to the trailing edges of

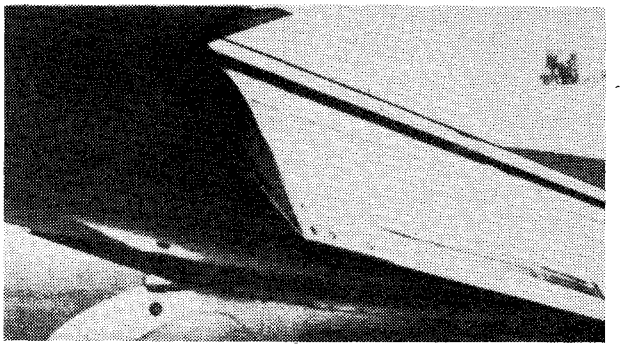

Fig. 3 Sensor array on HFB-320 flap side edge.

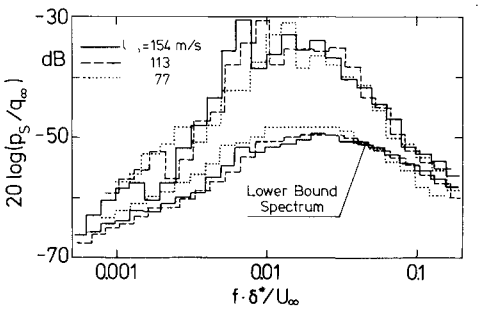

Fig. 4 Typical normalized surface pressure spectra as measured in cruise configuration near HFB-320 flap trailing edge.

both the HFB-320 and the DC-10/30, two typical spectral shapes were obvious. One, representing a lower bound, shows a very smooth "haystack" shape for a wide range of freestream velocities. The other contains superimposed discrete components whose frequencies are seemingly independent of freestream velocity. A comparison of both types of spectra on a nondimensional basis† shows generally higher pressure levels when discrete components are present (Fig. 4). With the exception of these discrete components, both cases show excellent normalization properties.

Obviously, the most severe deviation between both types of spectra (up to 15 dB) occurs within the Strouhal number range of maximum pressure intensities. No relationship between this phenomenon and a particular sensor location could be determined. However, while an influence of engine noise could be excluded on the basis of reference data obtained with the aircraft at rest and with the engines running, vibrational effects were clearly identified to be responsible for that phenomenon.

Vibration measurements in the vicinity of the respective sensor array showed that the acceleration level spectra exhibit a broadband character and are comparable to the surface pressure spectra. Evidently, vibration is driven by turbulent flow shedding off the trailing edge. However, since the wing surface is not rigid and only one vibration pickup was employed, only order-of-magnitude information of the vibrational wing surface response is obtained. Depending on panel thickness and driving frequency, but nearly independent of flow velocity, flow-excited bending waves must be expected[5,6] with wavelengths on the order of several centimeters, well within typical sensor separation distances. Analyses of phase spectra for different sensor pairs showed that flow-excited bending waves are indeed present. Unfortunately, the complex wing structure and the additional "spoiling" effect of the sensor plate itself (altering the local

†Fluctuating surface pressure referenced to freestream dynamic pressure vs a Strouhal number defined through the freestream velocity and the local boundary-layer displacement thickness.

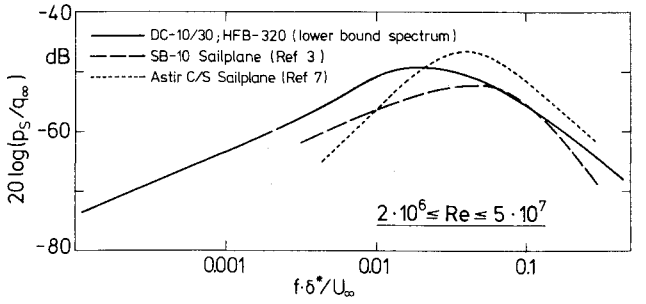

Fig. 5 Normalized surface pressure spectra near wing trailing edges of different aircraft.

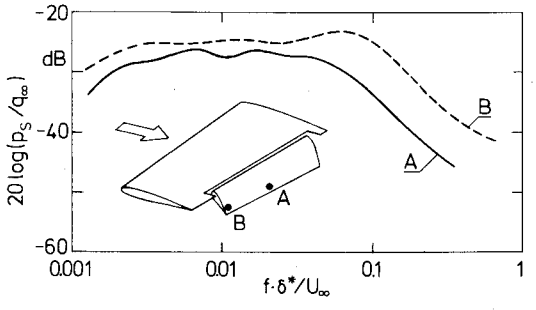

Fig. 6 Comparison of normalized surface pressure spectra measured near HFB-320 wing trailing edge at midspan location a) and near side edge b) with 50 deg flap deflection angle.

vibrational characteristics) prohibit the computation of the vibrational modes. To obtain more information on possible coupling processes between whole-wing vibration or localized surface vibration and fluctuating flow pressures, a controlled model experiment was conducted. A replica of a typical structural flap element was exposed to turbulent flow on one side. Discrete-frequency external vibrational excitation of that element caused a broadband increase of turbulent flow pressure levels. Thus, one could be fairly certain that both spectra presented in Fig. 4 do indeed represent the actual surface pressure characteristics.

To compare pressure data on real aircraft wings with data gathered under carefully controlled conditions and at significantly lower Reynolds numbers, pressure spectra representing the earlier defined lower bound are shown in Fig. 5 in a nondimensional representation together with surface pressure spectra obtained near the trailing edges of glider wings.[3,7] Considering the vastly different geometric scales, good agreement is achieved with respect to absolute levels and spectral shapes. In addition, the excellent fit between the low Strouhal number part (obtained by the upstream-located reference sensor at 30% of wing chord for the HFB-320) and the high Strouhal number part (as measured near the trailing edge), when compared on the basis of calculated boundary-layer displacement thickness, indicates the reliability of the procedure and the accuracy of the data.

Landing-Approach Configuration

For a flap deflection angle of 50 deg (corresponding to a landing-approach configuration) one finds a drastic increase in surface pressure intensities compared to those for the cruise configuration. The corresponding level difference is minimum at a Strouhal number of approximately 0.02, pertaining to the spectral peak at cruise configuration, and increases successively for higher and lower Strouhal numbers, respectively. The resulting extremely flat spectrum shape over a wide frequency range (Fig. 6) is typical for the separated flow conditions in the vicinity of the flap trailing edge for a 50 deg flap deflection angle. In accord with this finding, data obtained on the lower flap surface correspond to those for the

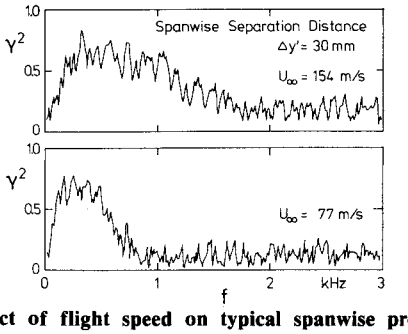

Fig. 7 Effect of flight speed on typical spanwise pressure field coherence spectra for cruise configuration.

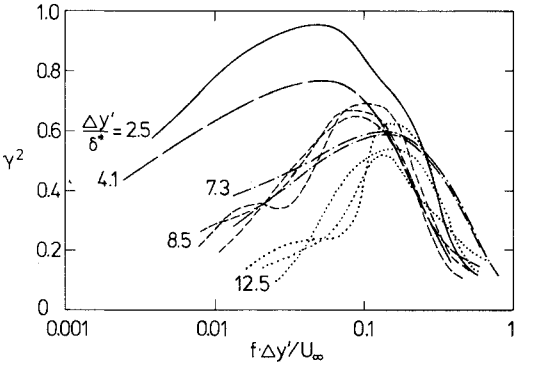

Fig. 8 Normalized HFB-320 and DC-10 spanwise surface pressure coherence spectra from measurements in cruise configuration for different flight speeds.

cruise configuration with the exception of a discrete low-frequency level increase due to the vibrational response to the flap.

Additional measurements were conducted on the HFB-320 at one side edge of the deflected flap; the results were compared to the spectrum as obtained at a near midspan location: For Strouhal numbers beyond 0.03 a drastic level increase of up to 10 dB was found due to the side-edge vortex that is driven by the steady-state pressure gradient between upper and lower flap surfaces.

Measurements at different chordwise locations along the side edge show the pressure levels to increase toward the upstream direction compared to a measurement position at the corner of side edge and flap trailing edge; this increase is due to the growing steady-state pressure differences in that direction. Within a distance from the side edge of about 30% of flap chord along the trailing edge, no substantial decrease in pressure level was detected; this finding indicates the substantial extent of three-dimensional flow phenomena and the ensuing importance for farfield-radiated total airframe noise.[8,9]

Pressure Field Coherence Data

As mentioned above, vibration effects on the surface pressures could be derived from coherence analyses and relevant phase spectra for certain sensor pairs. Since there is as yet no definite proof that vibrationally influenced pressures are always aerodynamical in nature—although that might be expected—the pressure field coherence analysis was limited to measurements pertaining to the "lower bound" pressure spectra.

Cruise Configuration

Typical plots of narrow band coherence spectra ($\Delta f = 12$ Hz) in the spanwise direction as measured at the suction side of the HFB-320 flap trailing edge appear in Fig. 7; as can be seen, maximum coherence shifts to higher frequencies with increasing the flow velocity.

As evident from Fig. 7 and from earlier measurements on glider wings[3] as well as from coherence data obtained by other investigators,[10] coherence spectra can be normalized on a Strouhal number basis. This is shown in Fig. 8 for pressure field coherences in the spanwise direction obtained for different sensor separation distances and flight speeds. While the high-frequency portions pertaining to different ratios of spanwise sensor separation distance and boundary-layer displacement thickness collapse fairly well, the low-frequency portions branch off at different Strouhal numbers depending on the particular ratio of $\Delta y'/\delta^*$. Similar results are obtained in the direction orthogonally to the trailing edge (Fig. 9). Since the coordinate x' has a predominant streamwise component with reference to the spanwise direction y', corresponding coherence values are higher with the maxima not as pronounced as in the spanwise direction.

Coherence spectra in Figs. 8 and 9 allow lines of constant $f\delta^*/U_\infty$ to be drawn as another parameter. This was done through graphical interpolation and some spectral smoothing. The results, as obtained in a spanwise direction for example, are shown in Fig. 10. Because of the few data available to date, the information is of tentative nature. In agreement with earlier analyses of comparable glider data an identical relationship is found between coherence and a Strouhal number, based on sensor separation distance for $f\delta^*/U_\infty \geq 0.04$ in the spanwise and orthogonal direction to the trailing edge. To deduce the integral pressure field correlation dimensions, the square root of the coherence function is plotted vs Strouhal number for the limiting case of $f\delta^*/U_\infty = 0.04$ in Fig. 11 and compared to data obtained from glider trailing-edge measurements and model experiments.[2,3] Obviously, the pressure field coherence as deduced from measurements on real aircraft wing/flaps is significantly higher. However, we must keep in mind that the comparison is not quite correct due to different coordinate systems used as a result of swept trailing edge.

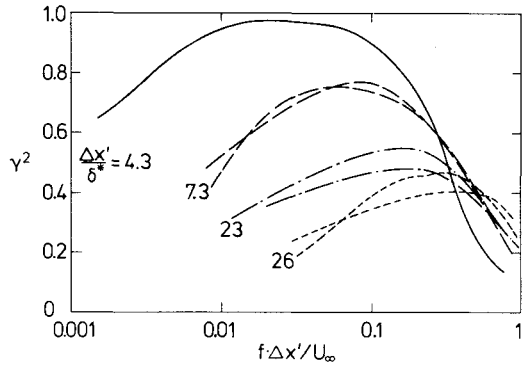

Fig. 9 Normalized HFB-320 and DC-10 surface pressure coherence spectra orthogonal to trailing edge from measurements in cruise configuration for different flight speeds.

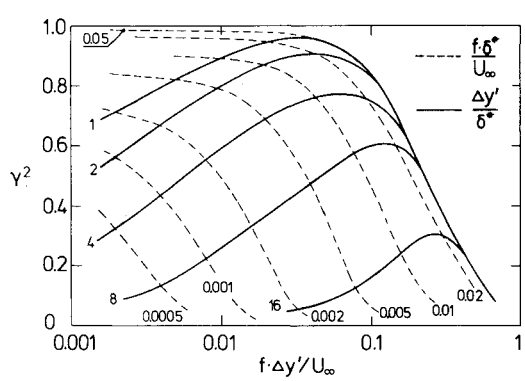

Fig. 10 Idealized normalized representation of spanwise surface pressure coherence for cruise configuration.

Integrating the continuously decreasing coherence coefficient γ vs Strouhal number based on sensor separation distance as given in Fig. 11 yields the pressure field correlation length scales of type

$$l_{x',y'} = C_{x',y'}\,(U_\infty/f) \qquad (1)$$

Applying this same procedure to different values of the parameter $(f\delta^*/U_\infty)$ as had been plotted in Fig. 10 for spanwise coherence, the variable C accounting for the flow characteristics is obtained as function of Strouhal number based on boundary-layer displacement thickness. This dependence is shown in Fig. 12 for spanwise direction and orthogonally to the trailing edge, exhibiting constant values for the respective flow parameters $C_{x'}$ and $C_{y'}$ for $f\delta^*/U_\infty \geq 0.04$ and a continuous decrease toward lower Strouhal numbers. Comparison with equally normalized surface pressure spectra shows the decrease of the flow variable C to occur at roughly that Strouhal number which pertains to the maximum pressure intensities when plotted in ⅓ octave bands (see Fig. 4).

To check integral correlation length scales as derived from present data against comparable results from glider measurements, one should account for the trailing-edge sweep angle. Assuming a correlation area of elliptic contour[11] with the larger axis in the streamwise direction and an axes ratio corresponding to C_x/C_y of 2.8 (as found on glider wings with the flow direction orthogonally to the trailing edge), one may compute the ratio of $C_{x'}/C_{y'}$ to be expected for the swept trailing edge, i.e., with a flow direction inclined by an angle of about 62 deg to the edge in the present case. The computed ratio of $C_{x'}/C_{y'} = 1.63$ is in excellent agreement with the ratio derived from present measurements $C_{x'}/C_{y'} = 1.65$ (see Fig. 12). Thus comparing correlation length scales on the basis of equivalent coordinate systems, they would be higher by a factor of 1.7 in the case of surface pressure fields near real aircraft trailing edges compared to those obtained on a glider trailing edge.

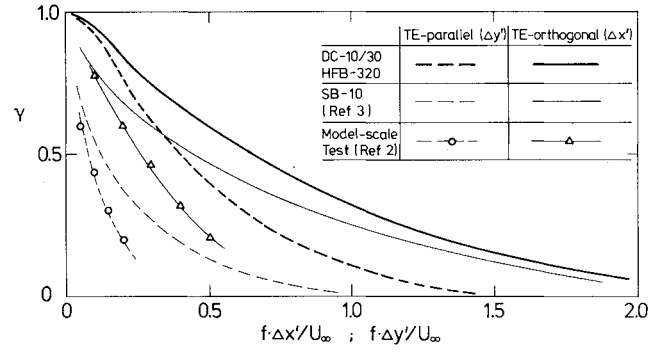

Fig. 11 Comparison of coherence properties for different flowfields in spanwise direction and orthogonal to trailing edge for $f\delta^*/U_\infty \geq 0.04$.

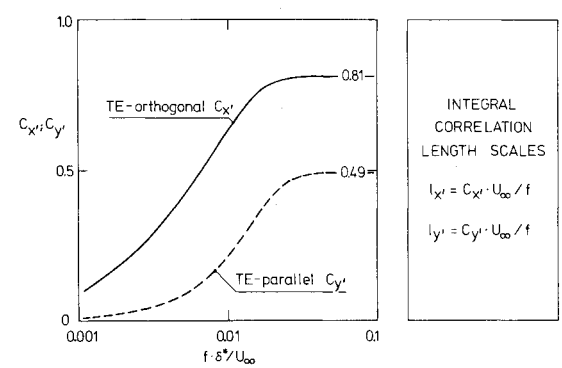

Fig. 12 Flow variables C as function of Strouhal number deduced from measurements in cruise configuration.

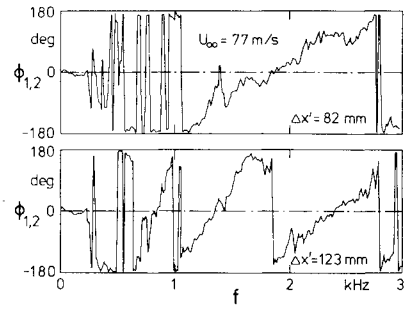

Fig. 13 Cross-power phase spectra from chordwise separated sensors at flap side edge for landing-approach configuration (50 deg flap deflection).

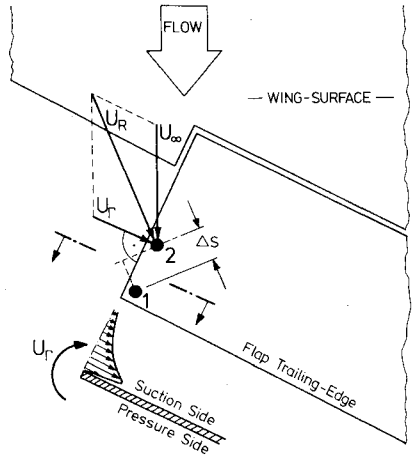

Fig. 14 Schematic plan view on flap side-edge geometry and corresponding flow pattern.

Landing-Approach Configuration

Spanwise coherence for a 50 deg flap deflection angle appears to be extremely broadband with no distinctly pronounced maximum. Furthermore, from cross-power phase spectra one finds a phase slope corresponding to a signal propagating from the wing tip with the speed of sound. Thus the outer flap side edge is assumed to be the origin of these sound signals. Evidently, coherence data comprise at least two phenomena with different coherence characteristics. Consequently, such a simple data reduction attempt as employed for the cruise configuration cannot be applied any longer. Furthermore, the flow separation near the edge gives rise to highly three-dimensional flow patterns. Data analyses are going on at present and no definite conclusion can be drawn as yet.

A few more details can be found, however, on the flow pattern at the flap side edge by phase analyzing signals from the sensors distributed along the flap side edge. From the example given in Fig. 13 which exhibits fairly clear phase slopes in the high-frequency range, one finds a convection speed significantly higher than the flight speed when based on a flow direction roughly corresponding to the direction of the potential flow. This finding holds for different sensor separation distances and flight speeds. A simple explanation is given by an additional velocity component originating from the side-edge vortex. Figure 14 represents a schematic plan view of the side-edge geometry considered and the respective velocity vectors. By an iterative process one can compute the approximate value of U_Γ necessary to produce the measured phase slope as a function of the sensor separation distance Δs and the velocity vector sum U_R. Through this procedure mean values of U_Γ were found to be on the order of 60-80% of the flight speed, the higher values pertaining to lower flight speeds due to the increasing lift coefficient. As indicated in

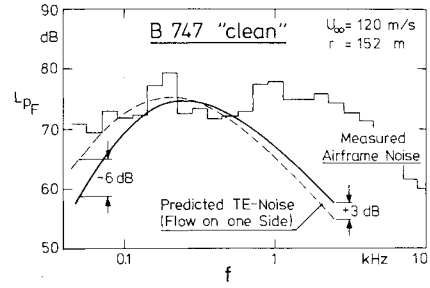

Fig. 15 Comparison of measured B747 airframe noise and trailing edge noise as predicted from hydrodynamic-edge noise model for cruise configuration.

Fig. 14 the velocity component U_Γ should be highest near the surface, decreasing continuously for increasing distance perpendicular to the flap surface. Thus for small-scale turbulence near the surface represented by higher fluctuating pressure frequencies, higher values of U_Γ are to be expected which result in a continuously decreasing slope of phase vs frequency. This effect was indeed found by phase analysis within a wide frequency range of 1-12 kHz for different sensor separation distances along the side edge (see Fig. 13). This frequency range corresponds to that where surface pressure intensities were found to be significantly higher compared to locations at large distances from the side edge (see Fig. 6).

Prediction of Trailing-Edge Noise from the Hydrodynamic Edge-Noise Model

A method to predict farfield-radiated trailing-edge noise from surface pressure characteristics at the edge is given by the hydrodynamic edge-noise model advanced by Hayden et al.[4]

In the case of the wing chord being large compared to the sound wavelength, and a flow Mach number below 0.5 (based on convection velocity) Hayden et al. derived a transfer function between farfield-radiated sound pressure and surface pressure for flow on one side of a semi-infinite plate. To check whether Hayden's model gives reasonable results in the case of trailing-edge noise radiation from a large commercial aircraft in the cruise configuration, data from the present study on surface pressure intensities and integral correlation length scales of the pressure field near the trailing edge are applied to Hayden's equation yielding the following transfer function:

$$\frac{\overline{p_F^2}}{\overline{p_S^2}} = \left(\frac{W}{4ar^2}\right)\left(\frac{l}{\xi}\right)U_\infty^2\left(\frac{l}{f}\right)C_x^{1/3}C_y^{5/3}\sin^2\theta\cos^2\left(\frac{\Psi}{2}\right) \quad (2)$$

From Eq. (2) a prediction of trailing-edge noise for a B747 commercial aircraft was carried out and the results compared to a measured airframe noise spectrum[12] for the cruise configuration (see Fig. 15). Following the arguments of Hayden et al. flow on both sides of the wing—not accounted for by Eq. (2)—results in a level increase of up to 3 dB for high Strouhal numbers and a decrease of 6 dB at low Strouhal numbers due to the respective covariances of fluctuating pressures from both sides of a plate/wing.

The comparison of predicted trailing-edge noise and measured airframe noise spectra exhibits fairly good agreement if trailing-edge noise is the main contributor to airframe noise and if one believes the effect of engine installation noise to be responsible for the high levels measured above 0.8 kHz, as has been stated by Fink.[13]

Measurements conducted with the same aircraft but with flaps deployed by 25 deg[12] exhibit a drastic increase in noise level compared to the cruise configuration. Since from the present investigation no significant effect on surface pressure

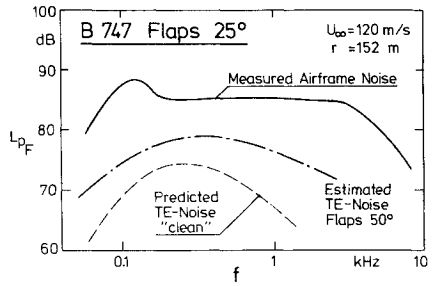

Fig. 16 Comparison of measured B747 airframe noise for 25 deg flap deflection angle and trailing-edge noise as predicted for cruise configuration and estimated for 50 deg flap deflection angle.

intensity or pressure field correlation dimensions could be detected for small flap deflection angles, the corresponding trailing-edge noise prediction would be identical to that valid for the cruise configuration (Fig. 16). Since trailing-edge noise scattering at the respective flap leading edges‡ is not likely to cause the broad 10–15 dB level increase, the question arises whether the hydrodynamic edge-noise model is generally incorrect or whether the mechanism of trailing-edge noise is masked by other more intense sources even for small flap deflection angles. To estimate the trailing-edge noise levels to be expected for the landing-approach configuration i.e., 50 deg flap deflection angle, on the basis of the hydrodynamic edge-noise model, a rough guess was made on the basis of data from the present study as presented in Fig. 16 for comparison. In contrary to the well-established experience that increasing the flap deflection angle generally results in an increase of the noise radiation, one finds that the corresponding spectrum would be even less intense than the measured 25 deg flap spectrum.

Conclusions

From surface pressure measurements near the trailing edges of real aircraft wings, a lower bound pressure intensity spectrum was deduced which is comparable to spectra pertaining to the flowfield near glider wing trailing edges at significantly lower Reynolds numbers. On the other hand, spectra were found that exhibited pronounced discrete components which cause a broadband level increase compared to that lower bound spectrum. This phenomenon was clearly tied to surface panel vibration. It can be expected that vibrational effects are the reason for higher integral correlation lengths as determined in the present study compared to those from "clean" experiments.

Making use of the hydrodynamic edge-noise model to predict the farfield-radiated trailing-edge noise for a commercial aircraft in cruise configuration provides reasonable agreement with measured data when the lower bound pressure spectrum and related integral pressure correlation scales are employed.

However, no definitive conclusion on the validity of the hydrodynamic-edge noise model can be drawn since its failure to predict airframe noise spectra for 25 deg flap deflection angle could have at least two reasons: First, the simple direct relation between surface and farfield-radiated pressure as postulated by the hydrodynamic model does not represent the dominating effect of edge noise radiation; and second, edge noise is not a dominant contributor to airframe noise even for small flap deflection angles. The latter assumption is supported by the obviously intense sound radiation from the flap side edges as could be deduced from measured data.

‡The assumption of edge noise radiation from a semi-infinite plate no longer holds.

Acknowledgments

The author would like to thank the Deutsche Lufthansa AG for the permission to conduct measurements on one of their DC-10/30 aircraft. Support given by Capt. H. Wissmann and his crew was greatly appreciated. Discussions on the aerodynamics of lifting flaps with A. Quast were useful for data interpretation. The author expresses his gratitude to H. Heller for his help in preparing the paper.

References

[1] Howe, M.S., "A Review of the Theory of Trailing Edge Noise," *Journal of Sound and Vibration,* Vol. 61, No. 3, 1978, pp. 437-465.

[2] Brooks, T.F. and Hodgson, T.H., "Investigation of Trailing-Edge Noise," *IUTAM/ICA/AIAA Symposium on Mechanics of Sound Generation in Flows,* Aug. 1979, Springer Verlag, Berlin and New York, 1979, pp. 76-84.

[3] Heller, H.H. and Dobrzynski, W.M., "Unsteady Surface Pressure Characteristics on Aircraft Components and Farfield Radiated Airframe Noise," *Journal of Aircraft,* Vol. 15, Dec. 1978, pp. 809-815.

[4] Hayden, R.E., Fox, H.L., and Chanaud, R.C., "Some Factors Influencing Radiation of Sound from Flow Interaction with Edges of Finite Surfaces," NASA CR-145073, 1976.

[5] Maestrello, L., "Measurement of Noise Radiated by Boundary Layer Excited Panels," *Journal of Sound and Vibration,* Vol. 2, No. 2, 1965, pp. 100-115.

[6] Maestrello, L., "Measurement and Analyses of the Response Field of Turbulent Boundary Layer Excited Panels," *Journal of Sound and Vibration,* Vol. 2, No. 3, 1965, pp. 270-292.

[7] Oas, S.C., "Glider Airframe Noise," AIAA Paper 79-0665, Seattle, Wash., March 1979.

[8] Kendall, J.M., "Airframe Noise Measurements by Acoustic Imaging," AIAA Paper 77-55, Los Angeles, Jan. 1977.

[9] Ahtye, W.F., Miller, W.R., and Meecham, W.C., "Wing and Flap Noise Measured by Near- and Far-Field Cross-Correlation Techniques," AIAA Paper 79-0667, Seattle, Wash., March 1979.

[10] Panton, R.L., "Theoretical and Flight Test Study of Pressure Fluctuations under a Turbulent Boundary Layer, Part 2: Flight Test Study," NASA CR-140448, 1974.

[11] Bull, M.K., "Properties of the Fluctuating Wall-Pressure Field of a Turbulent Boundary Layer," AGARD Rept. 455, Paris, 1963.

[12] Fink, M.R., "Airframe Flyover Noise Data Report," UTRC R77-912607-9, 1977.

[13] Fink, M.R., "Airframe Noise Prediction Method," FAA-RD-77-29, 1977.